Chinese Science Bulletin

Age and genesis of the Myanmar jadeite: Constraints from U-Pb ages and Hf isotopes of zircon inclusions

QIU ZhiLi[1,3], WU FuYuan[2†], YANG ShuFeng[3], ZHU Min[4], SUN JinFeng[2] & YANG Ping[5]

[1] Department of Earth Sciences, Sun Yat-sen University, Guangzhou 510275, China;
[2] State Key Laboratory of Lithospheric Evolution, Institute of Geology and Geophysics, Chinese Academy of Sciences, Beijing 100029, China;
[3] Department of Earth Sciences, Zhejiang University, Hangzhou 310027, China;
[4] Institute of Nonferrous Metal Geology of Guangdong, Guangzhou 510008, China

Myanmar jadeite (jadeitite) is well known for its economical value and distinctive tectonic locality within the collisional belt between India and Eurasian plates. However, it is less studied for its genesis and geodynamic implications due to precipitous topography, adverse weather and local military conflicts in the area. By means of combined ICP-MS and LA-MC-ICPMS techniques, we have carried out *in-situ* trace elements, U-Pb and Lu-Hf isotopes for zircon inclusions in a piece of jadeite gem sample. CL imaging suggests that the zircons are metasomatic in origin, and contain mineral inclusions of jadeite and omphacite. Seventy-five analyses on 16 grains of the zircons yield a U-Pb age of 158 ± 2 Ma. The Myanmar zircons differ from other types in that they have no significant Eu anomalies despite high HREE concentrations. Measured $^{176}Hf/^{177}Hf$ ratios range from 0.282976 to 0.283122, with an average value of 0.283066 ± 7; $\varepsilon_{Hf}(t)$ value of 13.8 ± 0.3 (n=75). These results indicate that the Myanmar jadeite was formed in the Late Jurassic, probably by interaction of fluid released from subducted oceanic slab with mantle wedge. Therefore, its formation has no genetic relationship to the continental collision between Indian and Euroasian plates.

Hafnium isotopes; U-Pb dating; zircon inclusion; Myanmar jadeite

Myanmar jadeite (jadeitite), located at the upper reach of the Uru River in north Myanmar, is globally known for its high quality in gemology. It is considered as the most typical type of precious jadeites in the global gem market. Due to the great economical value, much attention has been paid to the genesis and geodynamic significance of this type of jadeite[1–3]. However, this jadeite is limitedly studied because of complex topography, adverse weather, and frequent military conflicts in the area. Available studies are mainly focused on two aspects, formation age and mechanism[2,4–8]. As for the formation time, the suggested ages range from Precambrian to Cenozoic[5,9,10], which is mainly based on the indirect evidence since jadeite cannot be dated directly. For its genesis, the suggested schemes include those of magmatic, metamorphic, and fluid metasomatic, showing much divergence in opinion[2,4,5,8,10–12].

Recently, it was found that zircon inclusions occur in the Myanmar jadeite[13–16]. This provides an important object to study its genesis. Especially, Shi et al.[8] concluded that the jadeite was formed at 146.5 ± 3.4 Ma by dating the separated zircons. However, zircons separated from a grand jadeite sample are probably complicated in origin; it requires, therefore, additional work to ascertain whether this age can precisely constrain its formation time. In this paper, we present *in-situ* analytical data of REE, U-Pb and Hf isotopes for zircon inclusions within

Received June 3, 2008; accepted September 25, 2008;
published online November 11, 2008
doi: 10.1007/s11434-008-0490-3
†Corresponding author (email: wufuyuan@mail.igcas.ac.cn)
Supported by National Natural Science Foundation of China (Grant No. 40673039) and the Science Plan Foundation of Guangdong (Grant No. 2007B031200005)

a Myanmar gem jadeite, to provide tight constraints on formation time and mechanism, and then geodynamic process.

1 Sample and geological background

Myanmar jadeite is located within the Southeastern Asian block, which, however, is not consentaneous about its tectonic subdivisions. It is generally accepted that this block can be divided into three sub-units bounded by the Mogok and Naga Hill faults or belts (Figure 1)[3,17–21]. The Naga Hill belt, the boundary between the India plate and Indo-Burma terrane, corresponds to the Yarlung Zangbo suture in south Tibet of China. To east of the Mogok belt, the Shan-Thai terrane, correspondent to the Baoshan-Tengchong terrane in southwest China, is separated from the Simao terrane along the Changning-Menglian suture zone. The area bounded by the Mogok and Naga Hill belts, where the famous Myanmar jadeite is located[22], is named the Central Myanmar block (also named East Myanmar block), which is correspondent to the Lhasa block in south Tibet. Intensive striking-slip, after India-Asia collision during the Cenozoic resulted in the dextral Sagaing fault to the west of Mogok fault, and it is generally thought that the Sagaing fault connects southwards to the spreading ridge in the Andeman Sea[23].

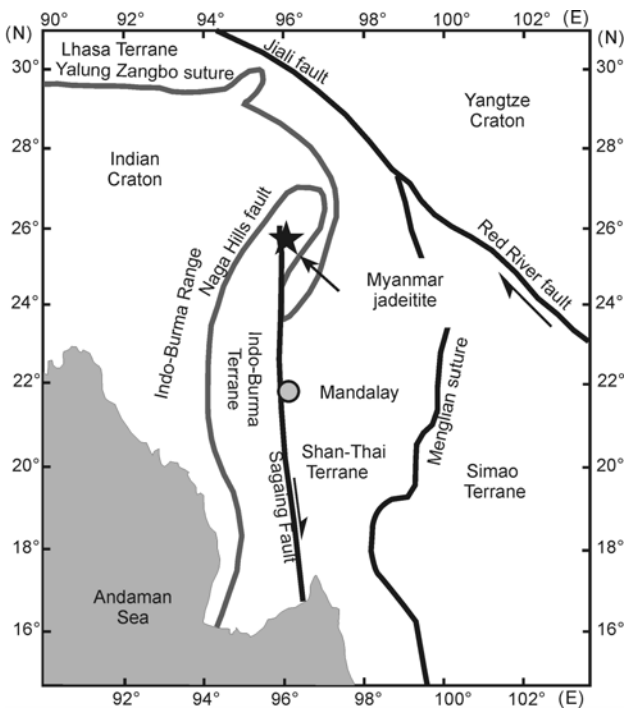

Figure 1 Simplified tectonic map showing location of the Myanmar jadeite.

Myanmar jadeite mostly occurs in the Hpakan area of the northern Central Myanmar block. It was thought sometimes that the Hpakan area is likely a part of the Sagaing tectonic belt in the north[3], or originally part of the Mogok belt, but was thrust later to the present location[21]. Jadeitite, primary rock of the Myanmar jadeite, occurred as veins within the serpentinized peridotite, which is surrounded by low-temperature and high-pressure metamorphic blue schist, mica schist, quartzite, amphibolite, marble, etc.[1,7,15,24].

The studied sample was collected from the famous Guangzhou jadeite market, where the jadeite articles are basically made of primary jadeite materials from Myanmar or Yunnan Province of China. The first author has observed thousands of jadeite articles using the 10 times magnifier, and has found that about ten of them contained zircon inclusions. The reason to select the studied sample for further works is that it contains the most abundant zircon inclusions. Meanwhile, the perfect crystal forms make this sample ideal to conduct various kinds of analyses.

Sample Jz0201, an apple-green jadeite article of "bean-green" type, is a typical jadeite variety. It is well polished into saddle-like shape for finger ring with size of 20 mm×9 mm×2 mm, refractive index of 1.66, and relative density of 3.33. In terms of gemology, Jz0201 is homogeneous in colour with crystalloblastic texture consisting of 0.2—1.0 mm jadeite mineral in grain-size, falling into "Douqing" type of high quality and popular jadeite category in the worldwide jadeite market[25]. On the polished surfaces, dozens of white zircon crystals occur in cluster or in multi-grain. Most zircons, displaying regular forms of tetragonal prism and bipyramid with length/width ratios of 1—3, range from 2 to 0.2 mm in grain-size, which makes it possible to conduct multiple analyses directly within the grain.

Although jadeite occurs in over 10 countries and districts, Myanmar is still the most important country for the global jadeite materials since it provides more than 98% quotient of total jadeite materials in the world. Moreover, Myanmar is the only location for occurrence of specious jadeite of high quality. In contrast to jadeites from other countries and areas, Myanmar jadeite of precious quality diagnostically consists of nearly pure (>98%) jadeite mineral[26,27]. In order to ascertain the original occurrence of our sample, electron microprobe was used to determine the chemical compositions (Table 1). Compared to jadeites in other areas, the low concen-

Table 1 Chemical comparisons of the studied jadeite of Jz0201 with those apple-green ones from other localities in the world

	This paper	Burma[28–31]	Guatemala[28,31]	Kazakhstan [32]	Russia[33,34]
Analyses	4	8	3	6	5
SiO_2	59.12	59.29	58.39	56.69	58.70
AL_2O_3	22.42	23.19	21.18	21.35	17.28
TiO_2	0.06	0.01	0.08	0.17	0.00
Fe_2O_3*	0.68	0.73	2.55	1.21	2.42
Cr_2O_3	0.05	0.10	~	0.16	0.68
MnO	0.02	0.01	0.06	0.01	0.10
MgO	1.45	1.39	1.86	2.12	3.62
CaO	2.19	1.77	2.59	2.83	5.33
Na_2O	13.19	13.40	12.92	13.54	11.50
K_2O	0.02	0.06	0.05	0.00	0.05
P_2O_5	0.03	0.00	0.08	–	–
Total	99.21	99.92	99.73	98.08	99.68

trations of Ca, Mg and Fe of the studied sample indicate that it is analogous to the Myanmar "Douqing" type in composition. Therefore, it is concluded that the studied sample came from northern Myanmar even though it was not personally collected from the field there.

2 Analytical methods

All analyses in this study were carried out at the State Key Laboratory of Lithoshperic Evolution, Institute of Geology and Geophysics, Chinese Academy of Sciences. CL images were obtained at CAMECA-SX-51 electron microprobe with 10 kV accelerative voltage. Trace elements, U-Pb and Hf isotopic compositions were determined in the MC-ICPMS (multi-collector inductively coupled plasma mass spectrometer) laboratory, which was equipped with Neptune MC-ICPMS, Agilent 7500a quadrupole ICPMS (Q-ICPMS), and 193 nm laser ablation system. All these machines have been previously introduced in relevant references[35–37].

Different from other analyses, the zircon U-Pb age, trace element and Hf isotopic data in this study were simultaneously determined. The applied laser beam is 60 μm in diameter with a frequency of 8 Hz and a model of spot ablation. The ablated materials were transported by He carrier gas through Y-type tube into Q-ICPMS and MC-ICPM machines, respectively. Standards of zircon 91500 and NIST SRM 610 were analyzed after every 5 sample analyses. Collection times of signal and gas background were 40 and 20 s, respectively. Isotopic ratios of $^{207}Pb/^{206}Pb$, $^{206}Pb/^{238}U$, $^{207}U/^{235}U$ ($^{235}U = {}^{238}U/137.88$) and $^{208}Pb/^{232}Th$ were calculated using GLITTER 4.0 software after fractionation correcting using zircon 91500 as external standard. During the error calculation of the isotope ratios, the standard deviation of the standard zircon 91500 and targeted samples have been considered, 2% standard deviation of the recommended isotopic values for 91500 has been merged as well. The weighted mean age and concordia diagram were carried out using Isoplot (ver 3.0) program. The concentrations of elements were calculated using GLITTER (ver 4.0) program with NIST SRM 610 as external and Si as internal standards.

Lu-Hf isotopic analyses were carried out using the Neptune MC-ICPMS according to the previously reported method[36], in which static signal collection was used with collection time of 30 s for background. The integration time was 0.131 s. Two hundred data sets were collected with an analytical duration of ~30 s. Interference of ^{176}Lu on ^{176}Hf was corrected using $^{175}Lu/^{176}Lu = 0.02655$ supposing that Lu has the same fractionation as that of Hf. Interference of ^{176}Yb on ^{176}Hf was corrected by measured Yb fractionation factor assuming $^{176}Yb/^{172}Yb = 0.5887$. During analyses, standard zircon 91500 was taken as external standard.

3 Analytical results

3.1 CL images of zircons and their genesis

Based on the observation under 10 times magnifier, twenty-five grains of zircon were identified on six sides of the sample (Figure 2), in which the biggest zircon has a length of 1.2 mm (Grain 23); whereas the smallest one is only 0.06 mm (Grain 19). However, most zircons range from 0.3 to 0.5 mm in length with a length/width ratio of 2—3.

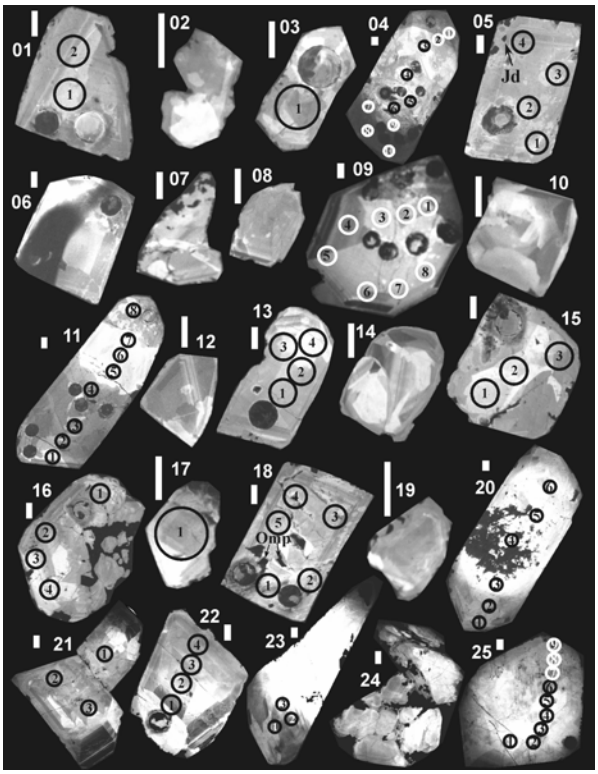

Figure 2 CL images of zircon crystals in Myanmar jadeite Jz0201. The white bar is 0.05 mm in length; unmarked round pits are positions of laser analyses before this study.

The CL images show that most zircons have regular forms and characteristic pyramid faces (Figure 2). However, it is noted that most zircons show heterogeneous cathodoluminescence with irregular and/or patchy internal structures, much different from those of the magmatic zircons. Moreover, minerals inclusions of jadeite and omphacite are also identified in grains 5 and 18. All of these observations suggest that the zircons were crystallized contemporaneously with the host jadeite, and genetically originated from fluid-induced metasomatism[1,38].

3.2 Rare earth elements of zircons

Although 25 grains of zircons have been identified in the sample, some of them cannot be analyzed directly since they are not exposed on the surface. The REE patterns of the sixteen analyzed zircons are shown in Figure 3(a). It is indicated that the zircons have large intra- and inter-grain variations for the REE concentrations although they are commonly depleted in LREE and enriched in HREE. Meanwhile, the studied zircons are different from those of magmatic by lack of negative Eu anomalies, and characterized by weak Ce positive anomalies and low HREE concentrations. The above-mentioned characteristics are much different from the magmatic zircons[39,40], but similar to those of hydrothermal origin, e.g. zircon 91500 in pegmatite[41,42].

Th concentrations of the studied zircons range from 0.4 to 163 ppm with most (90%) less than 10 ppm; U concentrations vary from 13 to 502 ppm, but mostly less than 100 ppm, which result in their low Th/U ratios of 0.01—0.34 with an average of ~0.10 (Figure 3(b)), consistent with the conclusion that the zircons are hydrothermal origin.

3.3 Zircon U-Pb isotopic analyses

U-Pb isotopic data of 75 analyses from the above 16 zircons are mainly located on the Concordia (Figure 4(a)), and have young and similar $^{206}Pb/^{238}U$ ages from 148 ± 12 to 189 ± 14 Ma with an average of 158 ± 2 Ma (Figure 4(b)). It was found that there is no correlation between the U-Pb age and Th/U ratio, suggesting that these zircons were crystallized from a common medium.

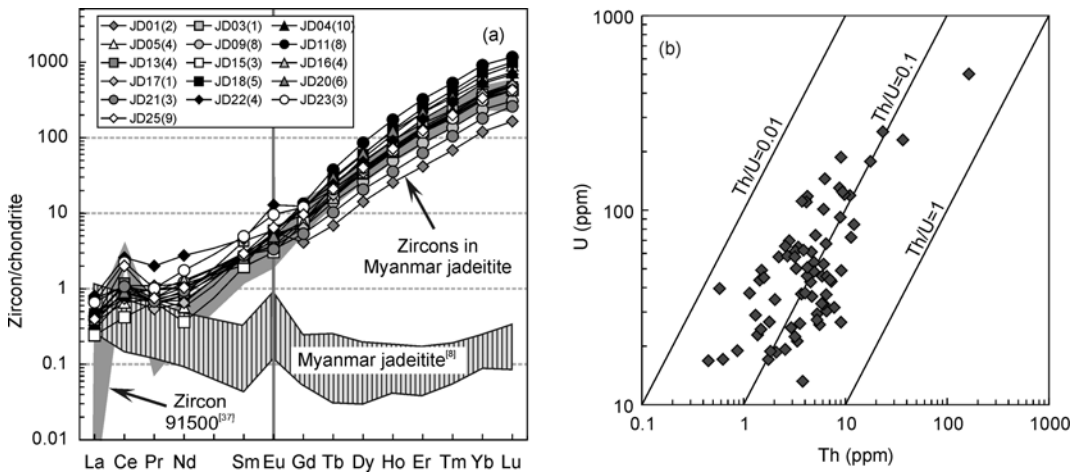

Figure 3 Chondrite-normalized REE patterns (a) and Th-U concentrations (b) of zircon inclusions in the Myanmar jadeite.

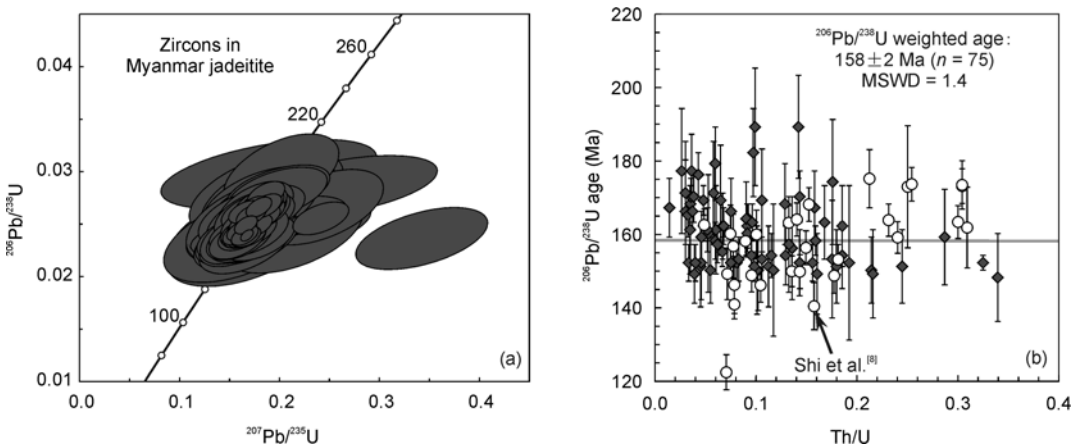

Figure 4 U-Pb age of zircons from the Myanmar jadeite (Jz0201).

Table 2 REE concentrations (ppm) of zircons in the Myanmar jadeite (Jz0201)

Analysis	La	Ce	Pr	Nd	Sm	Eu	Gd	Tb	Dy	Ho	Er	Tm	Yb	Lu
Jz0201 01(2)[a)]	0.21	0.90	0.12	0.70	0.40	0.41	1.06	0.34	4.62	1.89	8.89	2.19	24.9	5.33
Jz0201 03(1)	0.13	0.91	0.07	0.49	0.82	0.43	3.09	1.22	15.7	6.84	32.8	7.46	78.2	15.0
Jz0201 04(10)	0.11	0.76	0.08	0.42	0.51	0.31	2.10	0.91	13.0	5.62	29.4	7.22	79.7	16.9
Jz0201 05(4)	0.11	0.54	0.08	0.34	0.52	0.27	2.03	1.12	17.5	8.17	46.4	12.0	137	29.4
Jz0201 09(8)	0.13	0.90	0.09	0.73	0.53	0.40	1.67	0.69	8.54	3.66	18.2	4.36	49.1	9.88
Jz0201 11(8)	0.09	0.65	0.07	0.49	0.46	0.40	3.47	1.85	27.9	12.8	68.7	17.1	190	37.7
Jz0201 13(4)	0.13	0.96	0.08	0.53	0.46	0.33	2.05	0.83	10.8	4.74	25.3	6.19	70.8	15.1
Jz0201 15(3)	0.08	0.34	0.08	0.22	0.37	0.22	1.93	0.86	12.3	4.94	25.3	6.14	68.4	13.9
Jz0201 16(4)	0.14	0.87	0.10	0.77	0.57	0.36	1.97	0.79	11.2	4.93	27.3	6.65	75.2	15.3
Jz0201 17(1)	0.14	0.60	0.06	0.39	0.54	0.26	1.67	0.86	11.3	5.54	27.9	6.75	77.6	15.9
Jz0201 18(5)	0.15	0.66	0.11	0.62	0.52	0.40	3.06	1.38	19.4	9.46	52.3	13.5	153	32.2
Jz0201 20(6)	0.12	0.74	0.11	0.61	0.49	0.36	3.02	1.46	20.0	9.07	45.7	11.0	116	23.7
Jz0201 21(3)	0.23	0.87	0.08	0.56	0.53	0.24	1.39	0.50	6.70	2.64	13.4	3.36	37.5	8.41
Jz0201 22(4)	0.26	2.11	0.23	1.65	0.88	0.93	3.21	1.18	15.4	6.70	37.5	9.44	109	22.2
Jz0201 23(3)	0.21	1.82	0.11	1.05	0.95	0.69	3.11	1.02	13.0	5.02	25.1	5.81	65.1	13.6
Jz0201 25(9)	0.12	1.63	0.09	0.62	0.56	0.47	2.49	1.03	13.1	5.29	26.6	6.41	69.5	13.9

a) Number in the bracket represents analytical times.

3.4 Hf isotopes

Hafnium isotopic data are listed in Table 3. All studied zircons have a homogeneous Hf isotopic composition, with $^{176}Lu/^{177}Hf$ ratios of 0.00004—0.00107 and $^{176}Hf/^{177}Hf$ ratios of 0.282976—0.283122. The average $^{176}Hf/^{177}Hf$ value is 0.283066 ± 7 (Figure 5(a)), which is correspondent to $\varepsilon_{Hf}(t)$ = 13.8 ± 0.3 (n = 75) (Figure 5(b)). It is also noted that there is no correlation between Hf isotopic and Th/U ratios for the studied zircons (Figure 5(b)).

4 Discussions

4.1 Formation age of the Myanmar jadeite

Myanmar jadeite deposit is located within the collision zone between Indian and Asian plates, and associated with a series of high-pressure metamorphic rocks, which came to the conclusion that it might be genetically related to the India-Asia collision[3,9]. However, the solid constraints on its formation age are very limited. It has been stated in the former sections that the studied zircons in the jadeite are metasomatic in origin since they are regular in shape, but irregular in internal structure. Meanwhile, the mineral inclusions, jadeite and omphacite, indicate that the zircons were crystallized coevally to the host jadeite. Therefore, it is concluded that the Myanmar jadeite was formed in the Late Jurassic with an absolute age of 158 ± 2 Ma (Figure 4).

However, it was recently reported by SHRIMP analyses that three groups of zircon with different U-Pb ages have been identified in the Myanmar jadeite[8]. The Group-I zircons contain sodium-free and magnesium-rich mineral inclusions and show typical oscillatory growth zones with $^{206}Pb/^{238}U$ age of 163.2 ±3.3 Ma, which was thought to represent the time of host ultramafic rock or its serpentinization. The Group-II zircons occur as rims

Table 3 U-Pb isotopic data of zircons in the Myanmar jadeite (Jz0201)

Analysis	Th (ppm)	U (ppm)	Th/U	Isotopic ratios								Isotopic ages (Ma)							
				$^{207}Pb/^{206}Pb$	1σ	$^{207}Pb/^{235}U$	1σ	$^{206}Pb/^{238}U$	1σ	$^{208}Pb/^{232}Th$	1σ	$^{207}Pb/^{206}Pb$	1σ	$^{207}Pb/^{235}U$	1σ	$^{206}Pb/^{238}U$	1σ	$^{208}Pb/^{232}Th$	1σ
Jz0201 01-1	1.4	22.8	0.06	0.0511	0.0092	0.1979	0.0341	0.0281	0.0016	0.0131	0.0073	244	275	183	29	179	10	263	145
Jz0201 01-2	3.7	37.1	0.10	0.0490	0.0100	0.2010	0.0380	0.0298	0.0025	0.0083	0.0042	146	254	186	32	189	16	166	85
Jz0201 03-1	12	84.5	0.14	0.0489	0.0052	0.1801	0.0176	0.0267	0.0012	0.0049	0.0013	144	138	168	15	170	7	98	26
Jz0201 04-1	6.5	67.3	0.10	0.0484	0.0038	0.1605	0.0117	0.0241	0.0008	0.0065	0.0013	117	105	151	10	154	5	131	26
Jz0201 04-2	2.1	18.6	0.11	0.0481	0.0082	0.1570	0.0243	0.0237	0.0017	0.0136	0.0039	105	213	148	21	151	11	273	78
Jz0201 04-3	1.3	28.9	0.05	0.0507	0.0084	0.1659	0.0248	0.0238	0.0017	0.0102	0.0071	228	207	156	22	151	11	205	141
Jz0201 04-4	11	72.6	0.16	0.0504	0.0040	0.1657	0.0121	0.0239	0.0008	0.0074	0.0012	213	107	156	11	152	5	149	24
Jz0201 04-5	7.8	31.6	0.25	0.0506	0.0082	0.1653	0.0245	0.0237	0.0016	0.0060	0.0018	223	210	155	21	151	10	121	36
Jz0201 04-6	9.0	26.5	0.34	0.0519	0.0106	0.1656	0.0309	0.0232	0.0020	0.0048	0.0017	282	262	156	27	148	12	97	33
Jz0201 04-7	6.1	52.8	0.12	0.0488	0.0048	0.1628	0.0149	0.0242	0.0009	0.0096	0.0017	137	134	153	13	154	6	193	33
Jz0201 04-8	8.7	130	0.07	0.0482	0.0032	0.1617	0.0099	0.0244	0.0007	0.0119	0.0018	109	86	152	9	155	4	239	36
Jz0201 04-9	4.6	42.8	0.11	0.0491	0.0052	0.1622	0.0159	0.0240	0.0010	0.0078	0.0024	154	142	153	14	153	6	157	49
Jz0201 04-10	4.7	36.1	0.13	0.0489	0.0071	0.1628	0.0222	0.0242	0.0012	0.0089	0.0022	143	211	153	19	154	8	179	43
Jz0201 05-1	1.8	17.1	0.10	0.0506	0.0106	0.1641	0.0324	0.0235	0.0017	0.0114	0.0033	224	291	154	28	150	11	230	67
Jz0201 05-2	3.6	26.2	0.14	0.0493	0.0125	0.1665	0.0398	0.0245	0.0022	0.0069	0.0036	163	310	156	35	156	14	139	72
Jz0201 05-3	6.5	30.3	0.21	0.0549	0.0080	0.1782	0.0240	0.0236	0.0014	0.0082	0.0017	407	194	166	21	150	9	165	34
Jz0201 05-4	5.3	29.3	0.18	0.0507	0.0088	0.1652	0.0264	0.0236	0.0016	0.0072	0.0022	228	234	155	23	151	10	145	45
Jz0201 09-1	2.0	34.8	0.06	0.0489	0.0113	0.1813	0.0391	0.0270	0.0023	0.0148	0.0073	143	289	169	34	171	14	297	146
Jz0201 09-2	4.0	114	0.04	0.0476	0.0031	0.1733	0.0105	0.0265	0.0008	0.0127	0.0024	78	84	162	9	168	5	254	47
Jz0201 09-3	0.9	18.9	0.05	0.0480	0.0086	0.1570	0.0264	0.0238	0.0015	0.0166	0.0087	98	241	148	23	152	10	332	172
Jz0201 09-4	4.2	118	0.04	0.0504	0.0032	0.1852	0.0108	0.0267	0.0008	0.0105	0.0026	215	82	173	9	170	5	211	52
Jz0201 09-5	0.6	17.1	0.04	0.0514	0.0091	0.1972	0.0331	0.0279	0.0017	0.0168	0.0128	260	265	183	28	177	10	337	254
Jz0201 09-6	1.5	24.4	0.06	0.0494	0.0094	0.1723	0.0305	0.0253	0.0019	0.0074	0.0051	168	252	161	26	161	12	149	102
Jz0201 09-7	0.4	16.8	0.03	0.0486	0.0140	0.1862	0.0508	0.0278	0.0028	0.0103	0.0250	129	343	173	43	177	17	208	501
Jz0201 09-8	37	230	0.16	0.0484	0.0024	0.1657	0.0076	0.0249	0.0006	0.0079	0.0007	119	65	156	7	158	4	159	14
Jz0201 11-1	3.4	21.2	0.16	0.0494	0.0092	0.1776	0.0312	0.0262	0.0017	0.0087	0.0028	165	258	166	27	167	10	174	56
Jz0201 11-2	6.3	145	0.04	0.0489	0.0036	0.1856	0.0126	0.0276	0.0009	0.0229	0.0036	141	94	173	11	176	6	457	71
Jz0201 11-3	9.0	187	0.05	0.0490	0.0025	0.1790	0.0085	0.0266	0.0006	0.0087	0.0017	147	67	167	7	169	4	175	33
Jz0201 11-4	5.9	45.8	0.13	0.0484	0.0076	0.1753	0.0252	0.0263	0.0018	0.0118	0.0030	118	199	164	22	168	11	237	61
Jz0201 11-5	4.0	37.6	0.11	0.0494	0.0093	0.1808	0.0311	0.0266	0.0022	0.0130	0.0048	166	236	169	27	169	14	261	96
Jz0201 11-6	1.1	37.4	0.03	0.0495	0.0104	0.1770	0.0343	0.0260	0.0022	0.0062	0.0069	170	259	165	30	166	14	126	138
Jz0201 11-7	1.4	43.7	0.03	0.0503	0.0050	0.1796	0.0164	0.0260	0.0010	0.0097	0.0045	208	135	168	14	165	6	196	89
Jz0201 11-8	2.2	57.6	0.04	0.0493	0.0044	0.1813	0.0148	0.0268	0.0011	0.0077	0.0034	160	113	169	13	170	7	155	68
Jz0201 13-1	3.3	50.2	0.07	0.0657	0.0126	0.2409	0.0412	0.0266	0.0024	0.0684	0.0148	798	214	219	34	169	15	1337	279
Jz0201 13-2	3.4	64.5	0.05	0.0466	0.0114	0.1615	0.0365	0.0251	0.0025	0.0041	0.0049	30	265	152	32	160	16	82	99
Jz0201 13-3	2.7	58.1	0.05	0.0481	0.0051	0.1654	0.0162	0.0249	0.0012	0.0086	0.0039	103	133	155	14	159	7	173	79
Jz0201 13-4	11	119	0.09	0.0481	0.0030	0.1713	0.0099	0.0258	0.0007	0.0084	0.0013	102	82	161	9	164	4	169	26
Jz0201 15-1	1.8	26.6	0.07	0.0583	0.0118	0.2053	0.0399	0.0255	0.0014	0.0079	0.0021	542	423	190	34	162	9	159	43
Jz0201 15-2	0.6	39.6	0.01	0.0481	0.0063	0.1739	0.0215	0.0262	0.0012	0.0389	0.0131	105	190	163	19	167	8	771	255
Jz0201 15-3	4.1	110	0.04	0.0457	0.0032	0.1646	0.0107	0.0261	0.0007	0.0080	0.0027	-18	88	155	9	166	5	160	53
Jz0201 16-1	6.6	45.7	0.14	0.0507	0.0116	0.1670	0.0370	0.0239	0.0014	0.0075	0.0026	227	415	157	32	152	9	152	52
Jz0201 16-2	6.5	36.8	0.18	0.0643	0.0152	0.2136	0.0455	0.0241	0.0025	0.0161	0.0047	753	283	197	38	153	16	323	93
Jz0201 16-3	1.5	49.2	0.03	0.0504	0.0099	0.1873	0.0337	0.0270	0.0022	0.0537	0.0190	213	250	174	29	171	14	1057	365
Jz0201 16-4	1.6	45.1	0.04	0.0483	0.0087	0.1686	0.0279	0.0253	0.0018	0.0192	0.0102	116	231	158	24	161	12	384	201
Jz0201 17-1	6.1	32.9	0.19	0.0461	0.0089	0.1620	0.0290	0.0255	0.0018	0.0128	0.0049		329	152	25	162	11	257	97
Jz0201 18-1	3.2	22.4	0.14	0.0461	0.0177	0.1887	0.0712	0.0297	0.0022	0.0100	0.0080		628	176	61	189	14	200	160

(*To be continued on the next page*)

(*Continued*)

Analysis	Th (ppm)	U (ppm)	Th/U	Isotopic ratios								Isotopic ages (Ma)							
				$^{207}Pb/^{206}Pb$	1σ	$^{207}Pb/^{235}U$	1σ	$^{206}Pb/^{238}U$	1σ	$^{208}Pb/^{232}Th$	1σ	$^{207}Pb/^{206}Pb$	1σ	$^{207}Pb/^{235}U$	1σ	$^{206}Pb/^{238}U$	1σ	$^{208}Pb/^{232}Th$	1σ
Jz0201 18-2	2.9	24.9	0.12	0.0490	0.0163	0.1592	0.0497	0.0236	0.0028	0.0303	0.0091	147	379	150	44	150	18	604	179
Jz0201 18-3	1.8	18.8	0.10	0.0668	0.0164	0.2632	0.0620	0.0286	0.0019	0.0087	0.0016	832	520	237	50	182	12	175	33
Jz0201 18-4	2.6	19.2	0.13	0.0595	0.0181	0.2017	0.0589	0.0246	0.0020	0.0076	0.0027	584	590	187	50	157	13	153	54
Jz0201 18-5	4.2	45.9	0.09	0.0684	0.0059	0.2405	0.0184	0.0255	0.0010	0.0118	0.0030	882	93	219	15	162	6	237	59
Jz0201 20-1	5.9	33.1	0.18	0.0498	0.0126	0.1881	0.0444	0.0274	0.0026	0.0123	0.0041	183	312	175	38	174	17	248	82
Jz0201 20-2	3.8	13.2	0.29	0.0484	0.0121	0.1666	0.0392	0.0250	0.0021	0.0080	0.0023	118	304	156	34	159	13	161	45
Jz0201 20-3	3.7	111	0.03	0.0494	0.0041	0.1627	0.0124	0.0239	0.0008	0.0120	0.0037	164	111	153	11	152	5	242	74
Jz0201 20-4	4.9	54.0	0.09	0.0475	0.0069	0.1684	0.0226	0.0257	0.0015	0.0107	0.0033	72	189	158	20	164	10	215	66
Jz0201 20-5	9.8	120	0.08	0.0512	0.0038	0.1686	0.0116	0.0239	0.0008	0.0076	0.0015	249	101	158	10	152	5	154	30
Jz0201 20-6	9.1	48.9	0.19	0.0518	0.0076	0.1728	0.0234	0.0242	0.0015	0.0136	0.0026	277	193	162	20	154	9	273	52
Jz0201 21-1	4.6	61.0	0.08	0.0492	0.0064	0.1776	0.0212	0.0261	0.0014	0.0087	0.0029	158	173	166	18	166	9	175	58
Jz0201 21-2	6.1	101	0.06	0.0512	0.0035	0.1751	0.0111	0.0248	0.0007	0.0131	0.0023	248	91	164	10	158	5	263	46
Jz0201 21-3	3.2	61.6	0.05	0.0488	0.0043	0.1708	0.0139	0.0253	0.0009	0.0128	0.0032	139	119	160	12	161	6	257	64
Jz0201 22-1	7.3	43.0	0.17	0.0499	0.0077	0.1763	0.0252	0.0256	0.0015	0.0061	0.0017	191	211	165	22	163	10	123	34
Jz0201 22-2	5.6	25.8	0.22	0.0513	0.0113	0.1659	0.0343	0.0234	0.0019	0.0140	0.0030	256	295	156	30	149	12	281	60
Jz0201 22-3	5.3	27.3	0.19	0.0513	0.0181	0.1697	0.0556	0.0239	0.0033	0.0073	0.0048	255	399	159	48	152	21	146	97
Jz0201 22-4	4.9	48.4	0.10	0.1048	0.0157	0.3416	0.0434	0.0236	0.0020	0.1040	0.0133	1711	120	298	33	150	12	2000	243
Jz0201 23-1	5.1	74.5	0.07	0.0504	0.0042	0.1770	0.0139	0.0254	0.0009	0.0124	0.0024	213	117	166	12	162	5	249	47
Jz0201 23-2	23	254	0.09	0.0480	0.0036	0.1662	0.0113	0.0251	0.0008	0.0105	0.0016	98	95	156	10	160	5	211	31
Jz0201 23-3	18	178	0.10	0.0510	0.0030	0.1671	0.0091	0.0237	0.0006	0.0097	0.0012	239	77	157	8	151	4	196	25
Jz0201 25-1	163	502	0.33	0.0505	0.0014	0.1667	0.0042	0.0239	0.0004	0.0080	0.0003	220	31	157	4	152	2	160	5
Jz0201 25-2	8.9	92.0	0.10	0.0513	0.0038	0.1812	0.0123	0.0256	0.0008	0.0070	0.0014	255	99	169	11	163	5	141	29
Jz0201 25-3	9.4	124	0.08	0.0500	0.0030	0.1646	0.0090	0.0239	0.0006	0.0091	0.0014	193	78	155	8	152	4	183	27
Jz0201 25-4	7.1	43.9	0.16	0.0489	0.0087	0.1580	0.0259	0.0234	0.0017	0.0062	0.0023	142	233	149	23	149	11	125	45
Jz0201 25-5	4.2	50.8	0.08	0.0491	0.0044	0.1627	0.0135	0.0240	0.0009	0.0093	0.0021	154	120	153	12	153	6	186	42
Jz0201 25-6	3.9	62.3	0.06	0.0490	0.0044	0.1672	0.0138	0.0247	0.0009	0.0093	0.0024	147	122	157	12	157	5	188	48
Jz0201 25-7	3.2	57.6	0.06	0.0489	0.0072	0.1595	0.0217	0.0236	0.0014	0.0114	0.0045	144	198	150	19	150	9	229	90
Jz0201 25-8	2.8	69.6	0.04	0.0497	0.0042	0.1643	0.0128	0.0239	0.0009	0.0108	0.0034	182	112	154	11	152	5	216	69
Jz0201 25-9	2.6	65.3	0.04	0.0486	0.0063	0.1573	0.0187	0.0234	0.0012	0.0110	0.0046	129	170	148	16	149	8	222	92

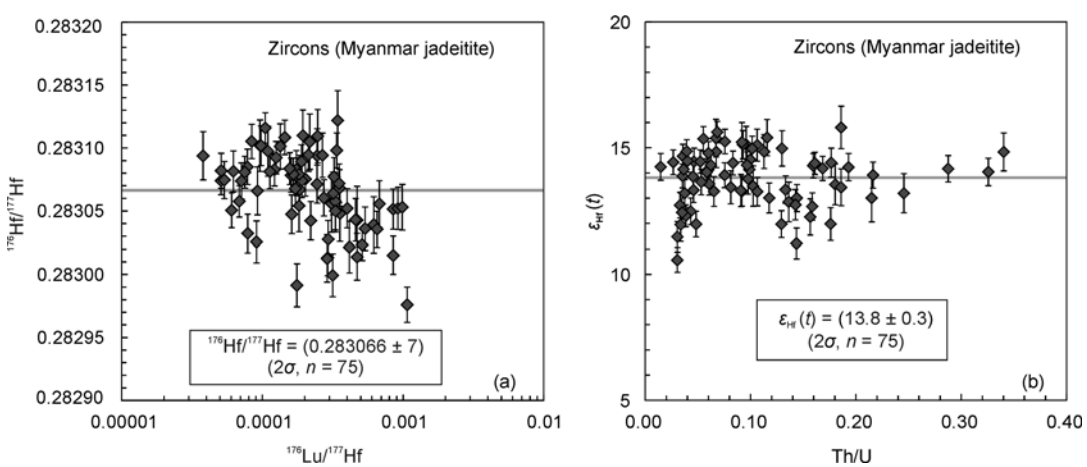

Figure 5 Lu-Hf isotopes of zircons in the Myanmar jadeite (Jz0201).

Table 4 Lu-Hf isotopic data of zircons in the Myanmar jadeite (Jz0201)

Analysis	$^{176}Yb/^{177}Hf$	$^{176}Lu/^{177}Hf$	$^{176}Hf/^{177}Hf$	2σ	$\varepsilon_{Hf}(0)$	$\varepsilon_{Hf}(t)$	2σ	T_{DM}	$f_{Lu/Hf}$
Jz0201 01-1	0.001416	0.000071	0.283074	0.000014	10.67	14.14	0.51	246	−1.00
Jz0201 01-2	0.001605	0.000078	0.283085	0.000014	11.07	14.53	0.50	230	−1.00
Jz0201 03-1	0.004954	0.000220	0.283042	0.000015	9.56	13.01	0.54	291	−0.99
Jz0201 04-1	0.001799	0.000096	0.283102	0.000020	11.67	15.13	0.72	207	−1.00
Jz0201 04-2	0.000780	0.000038	0.283094	0.000019	11.38	14.85	0.67	218	−1.00
Jz0201 04-3	0.001945	0.000092	0.283066	0.000019	10.39	13.86	0.67	257	−1.00
Jz0201 04-4	0.008932	0.000415	0.283022	0.000020	8.82	12.25	0.72	321	−0.99
Jz0201 04-5	0.008024	0.000356	0.283048	0.000022	9.76	13.20	0.78	284	−0.99
Jz0201 04-6	0.005236	0.000245	0.283094	0.000021	11.38	14.83	0.75	219	−0.99
Jz0201 04-7	0.004020	0.000194	0.283110	0.000020	11.95	15.41	0.72	196	−0.99
Jz0201 04-8	0.005156	0.000247	0.283109	0.000021	11.93	15.38	0.75	197	−0.99
Jz0201 04-9	0.002741	0.000134	0.283101	0.000018	11.65	15.11	0.63	208	−1.00
Jz0201 04-10	0.002147	0.000109	0.283098	0.000020	11.51	14.97	0.70	213	−1.00
Jz0201 05-1	0.006303	0.000310	0.283056	0.000023	10.04	13.48	0.80	272	−0.99
Jz0201 05-2	0.012706	0.000619	0.283039	0.000022	9.45	12.85	0.79	298	−0.98
Jz0201 05-3	0.009640	0.000472	0.283043	0.000027	9.58	13.00	0.94	292	−0.99
Jz0201 05-4	0.006727	0.000329	0.283058	0.000023	10.10	13.54	0.81	270	−0.99
Jz0201 09-1	0.005020	0.000245	0.283071	0.000015	10.59	14.03	0.54	250	−0.99
Jz0201 09-2	0.004164	0.000185	0.283067	0.000013	10.43	13.89	0.47	256	−0.99
Jz0201 09-3	0.001312	0.000060	0.283051	0.000014	9.85	13.32	0.49	278	−1.00
Jz0201 09-4	0.004252	0.000190	0.283089	0.000013	11.22	14.67	0.47	225	−0.99
Jz0201 09-5	0.001135	0.000051	0.283074	0.000011	10.68	14.15	0.39	245	−1.00
Jz0201 09-6	0.001527	0.000068	0.283058	0.000013	10.10	13.57	0.44	268	−1.00
Jz0201 09-7	0.001104	0.000051	0.283082	0.000014	10.96	14.43	0.49	234	−1.00
Jz0201 09-8	0.003710	0.000160	0.283078	0.000014	10.84	14.29	0.48	240	−1.00
Jz0201 11-1	0.001741	0.000079	0.283032	0.000015	9.20	12.67	0.54	303	−1.00
Jz0201 11-2	0.006937	0.000294	0.283028	0.000015	9.04	12.48	0.52	312	−0.99
Jz0201 11-3	0.007121	0.000291	0.283013	0.000014	8.54	11.98	0.51	332	−0.99
Jz0201 11-4	0.018134	0.000851	0.283015	0.000015	8.60	11.98	0.53	334	−0.97
Jz0201 11-5	0.018093	0.000851	0.283051	0.000016	9.88	13.27	0.56	282	−0.97
Jz0201 11-6	0.022990	0.001069	0.282976	0.000014	7.21	10.57	0.49	392	−0.97
Jz0201 11-7	0.014271	0.000654	0.283036	0.000014	9.32	12.73	0.51	303	−0.98
Jz0201 11-8	0.011196	0.000512	0.283023	0.000012	8.89	12.31	0.44	319	−0.98
Jz0201 13-1	0.006678	0.000331	0.283050	0.000017	9.83	13.27	0.59	281	−0.99
Jz0201 13-2	0.005538	0.000273	0.283060	0.000014	10.20	13.64	0.51	266	−0.99
Jz0201 13-3	0.003526	0.000174	0.283083	0.000015	11.00	14.45	0.53	233	−0.99
Jz0201 13-4	0.001996	0.000098	0.283102	0.000016	11.66	15.13	0.56	207	−1.00
Jz0201 15-1	0.005311	0.000267	0.283094	0.000018	11.40	14.84	0.62	218	−0.99
Jz0201 15-2	0.003685	0.000176	0.283077	0.000015	10.79	14.25	0.53	242	−0.99
Jz0201 15-3	0.003668	0.000161	0.283047	0.000015	9.74	13.20	0.54	283	−1.00
Jz0201 16-1	0.003940	0.000176	0.282991	0.000017	7.76	11.21	0.60	361	−0.99
Jz0201 16-2	0.009898	0.000472	0.283014	0.000018	8.55	11.98	0.65	332	−0.99
Jz0201 16-3	0.006528	0.000316	0.282999	0.000017	8.04	11.48	0.60	351	−0.99
Jz0201 16-4	0.002038	0.000091	0.283026	0.000016	8.97	12.43	0.58	313	−1.00
Jz0201 17-1	0.007131	0.000343	0.283122	0.000024	12.37	15.81	0.84	180	−0.99
Jz0201 18-1	0.011280	0.000537	0.283036	0.000017	9.34	12.75	0.61	302	−0.98
Jz0201 18-2	0.009442	0.000460	0.283043	0.000017	9.58	13.01	0.59	291	−0.99
Jz0201 18-3	0.006643	0.000320	0.283064	0.000017	10.32	13.76	0.60	261	−0.99
Jz0201 18-4	0.008344	0.000401	0.283052	0.000016	9.90	13.34	0.55	278	−0.99
Jz0201 18-5	0.019214	0.000919	0.283052	0.000017	9.90	13.28	0.59	282	−0.97
Jz0201 20-1	0.001293	0.000062	0.283081	0.000016	10.94	14.41	0.57	235	−1.00
Jz0201 20-2	0.001135	0.000054	0.283075	0.000015	10.70	14.17	0.52	245	−1.00
Jz0201 20-3	0.006759	0.000289	0.283013	0.000019	8.51	11.95	0.66	333	−0.99
Jz0201 20-4	0.020099	0.000987	0.283053	0.000018	9.94	13.31	0.64	281	−0.97
Jz0201 20-5	0.015113	0.000679	0.283056	0.000018	10.03	13.43	0.65	275	−0.98

(*To be continued on the next page*)

(*Continued*)

Analysis	$^{176}Yb/^{177}Hf$	$^{176}Lu/^{177}Hf$	$^{176}Hf/^{177}Hf$	2σ	$\varepsilon_{Hf}(0)$	$\varepsilon_{Hf}(t)$	2σ	T_{DM}	$f_{Lu/Hf}$
Jz0201 20-6	0.004086	0.000182	0.283054	0.000021	9.98	13.43	0.73	274	–0.99
Jz0201 21-1	0.001701	0.000084	0.283105	0.000014	11.79	15.25	0.48	202	–1.00
Jz0201 21-2	0.002430	0.000125	0.283092	0.000013	11.33	14.79	0.46	220	–1.00
Jz0201 21-3	0.002599	0.000122	0.283083	0.000013	10.99	14.45	0.46	233	–1.00
Jz0201 22-1	0.004210	0.000202	0.283075	0.000014	10.73	14.18	0.48	244	–0.99
Jz0201 22-2	0.007407	0.000353	0.283068	0.000015	10.48	13.91	0.51	255	–0.99
Jz0201 22-3	0.006771	0.000323	0.283077	0.000015	10.79	14.23	0.54	243	–0.99
Jz0201 22-4	0.007014	0.000337	0.283098	0.000014	11.53	14.97	0.49	213	–0.99
Jz0201 23-1	0.002040	0.000105	0.283116	0.000012	12.16	15.63	0.43	187	–1.00
Jz0201 23-2	0.004781	0.000217	0.283105	0.000022	11.78	15.23	0.78	203	–0.99
Jz0201 23-3	0.004084	0.000191	0.283074	0.000014	10.69	14.14	0.48	246	–0.99
Jz0201 25-1	0.008685	0.000351	0.283072	0.000015	10.60	14.04	0.54	250	–0.99
Jz0201 25-2	0.003920	0.000182	0.283079	0.000015	10.86	14.32	0.53	239	–0.99
Jz0201 25-3	0.003679	0.000172	0.283068	0.000014	10.46	13.91	0.49	255	–0.99
Jz0201 25-4	0.001673	0.000075	0.283081	0.000013	10.92	14.39	0.45	236	–1.00
Jz0201 25-5	0.002385	0.000113	0.283081	0.000013	10.94	14.40	0.48	236	–1.00
Jz0201 25-6	0.003506	0.000166	0.283079	0.000013	10.86	14.32	0.46	239	–0.99
Jz0201 25-7	0.003003	0.000145	0.283108	0.000014	11.90	15.36	0.48	198	–1.00
Jz0201 25-8	0.003255	0.000156	0.283084	0.000013	11.02	14.48	0.45	232	–1.00
Jz0201 25-9	0.004426	0.000212	0.283095	0.000013	11.41	14.86	0.46	217	–0.99

around those of the Group-I with $^{206}Pb/^{238}U$ age of 146.5 ± 3.4 Ma. Considering that these zircons do not show any internal growth zones and have low Th/U ratios, 146.5 ± 3.4 Ma was considered as the metamorphic time, hence the age of jadeite. The Group-III zircons have the lowest Th/U ratios and occur across zircons of the former two groups. The single analysis gives a $^{206}Pb/^{238}U$ age 122.2 ± 4.8 Ma, which was considered to represent the time of later thermal event after the formation of jadeite. However, our analyses yield different results. Firstly, we did not obtain any age of ca. 122 Ma even though our ages show some variations. It is noted that the Group-III zircon reported by Shi et al.[8] displays a similar feature of fluid infiltration to grain 15 in this study. However, two analyses on our grain yield identical ages of 162 ± 9 and 167 ± 8 Ma, respectively, consistent with the ages of other grains. Secondly, our study shows that the zircons do not show clear oscillatory zones and there is no correlation between the U-Pb ages and Th/U ratios. Considering that zircons rarely occur in ultramafic rocks due to their low concentrations of zirconium, it is suggested that all zircons reported by Shi et al.[8] were metasomatic by fluid since oscillatory zones can occasionally developed in the hydrothermal zircons[43,44]. If we re-calculate the data reported by Shi et al.[8] except the youngest age of 122.2 ± 4.8 Ma, the obtained weighted mean age is 157 ± 4 Ma, identical to our age of 158 ± 2 Ma. Considering that our studied sample Jz0201 is one kind of precious jadeite of "apple-green" type, our age of 158 ± 2 Ma obtained directly from zircons within the jadeite should better represent the age of the precious jadeite ore body in Myanmar.

The above age provides an important constraint on the geodynamic setting in which the Myanmar jadeite occurs. According to the updated data summary[45], the collision between the Indian and Asian plates most probably took place around 55 Ma, which indicates that the formation of the Myanmar jadeite is not genetically related to the India-Asia collision.

4.2 Constraint of zircon Hf isotopes on genesis of the Myanmar jadeite

Jadeite is generally considered as a typical mineral crystallized during the low-temperature/high-pressure metamorphism. Although jadeite can remain stable within broad ranges of temperature and pressure, it is commonly accepted that most jadeites are developed under high pressure[27]. However, jadeites are generally characterized by vein occurrence, enrichment of LREE and LILs (e.g. Li, Ba, Sr), and depletion in HFSE, suggesting that their formation are closely associated with fluid although the nature of this fluid is not clearly understood[2,26,46,47].

Zircon is a main mineral containing Hf element. For igneous rocks, the Hf isotopic compositions can provide valuable information to constrain the nature of the magmatic source from which zircon crystallized[48]. For hydrothermal or metasomatic zircon, however, the geo-

chemical interpretation of its Hf isotopic compositions is necessarily dependent on the specific mechanism the zircon formed[49]. The studied zircons have regular shape and have been identified as metasomatic hydrothermal origin, their Hf isotopes thus can shed light to the nature of the metasomatic fluid. Firstly, the average $^{176}Hf/^{177}Hf$ ratio of 0.283066 ± 7 and $\varepsilon_{Hf}(t)$ value of 13.8 ± 0.3 are similar to those of the depleted mantle or juvenile oceanic crust. Secondly, the $^{176}Lu/^{177}Hf$ ratios of 0.00004—0.00107 are much higher than those of zircons crystallized from garnet-bearing rocks, indicating that the fluid came from a source without garnet residue. It has been previously stated that the Myanmar jadeites mainly occur as tectonic lens, irregular small blocks and/or veins in strongly serpentinized ultramafic rocks, and the jadeite itself shows complex growth patterns for its internal structure. Combining with recently obtained data from fluid inclusions, trace elements and oxygen isotopes, therefore, it is proposed that this fluid was formed by dehydration of subducted oceanic slab, which implies that oceanic subduction is probably the first important tectonic setting in which the Myanmar jadeites were formed.

In view of the field geology, the Myanmar jadeite occurs within the central Myanmar block, bounded by the Mogok and Naga Hill belts. The wall rocks are mainly serpentitized peridotite, whose geodynamic implications remain questionable although it has been considered as parts of an ophiolite suite. The updated studies[3,18], however, displayed that there is no evidence for occurrence of ophiolite in the Mogok area[3], and that only sporadic magmatism of the Middle Jurassic (~170 Ma) has been identified in the limited rocks[18]. Most rocks in the area were formed and later deformed during the Cenozoic. Therefore, the formation of Myanmar jadeite is not related to the Mogok belt.

However, Late Triassic flysch, Jurassic ophiolite and siliceous rocks have been found along the Kath-Gangaw mountain range to north of the Mogok belt[21]. These rocks, generally unconformably overlaid by Late Cretaceous-Paleogene marine sedimentary rocks, can be traced continuously to the Naga Hill area to west of the Myanmar jadeite deposit, and extend further southward along the India-Burma Range. It is speculated that the above belt should be correlated to the Yarlung Zangbo suture in Tibet[3,21], but the later tectonic processes modified the occurrence of an originally coherent belt (Figure 1), and the poor rock exposure makes its geological history less known [20,21], since the limited researches are mostly focused on the Cenozoic geology with much less knowledge on the early geological evolution. However, the present study suggests that this belt began its oceanic subduction at least since 158 Ma, consistent with finding of the Jurassic magmatism in Gangdese of the south Tibet[50,51]. Therefore, subduction of the Neo-Tethysan Ocean between India and Asia took place much earlier than we previously thought.

5 Conclusions

(1) Studies of zircons within a jadeite article showed that the main ore body of precious Myanmar jadeite was formed during the Late Jurassic with an age of 158 ± 2 Ma. It is indicated that formation of the Myanmar jadeite was not associated with the Cenozoic collision between Indian and Asian plates;

(2) The main ore body of precious Myanmar jadeite was originated from fluid-induced metasomatism. Zircon Hf isotopic data further inferred that this fluid was related to dehydration of subducted oceanic slab.

1 Corfu F, Hanchar J M, Hoskin P W O, et al. Atlas of zircon textures. In: Hanchar J M, Hoskin P W O, eds. Zircon. Rev Mineral Geochem, 2003, 53: 468—500

2 Sorensen S, Harlow G E, Rumble D. The origin of jadeitite-forming subduction-zone fluids: CL-guided SIMS oxygen-isotope and trace-element evidence. Am Mineral, 2006, 91: 979—996[DOI]

3 Searle M P, Noble S R, Cottle J M, et al. Tectonic evolution of the Mogok metamorphic belt, Burma (Myanmar) constrainted by U-Th-Pb dating of metamorphic and magmatic rocks. Tectonics, 2007, 26: 2006TC002083

4 Cui W Y, Shi G H, Yang F X, et al. A new viewpoint—magma genesis of jadeite Jade (in Chinese). J Gems Gemmol, 2000, 2: 16—22

5 Zhou Z Y, Liao Z T, Xu Y M. The new genesis model of jadeite in Burma (in Chinese). Shanghai Geol, 2005, 93(1): 58—61

6 Harlow G E, Sorensen S S. Jade: occurrence and metasomatic origin. Aust Gem, 2001, 21: 7—10

7 Shi G H, Cui W Y, Tropper P, et al. The petrology of a complex sodic and sodic-calcic amphibole association and its implications for the metasomatic processes in the jadeitite area in northwestern Myanmar, formerly Burma. Contrib Mineral Petrol, 2003, 145: 355—376[DOI]

8 Shi G H, Cui W Y, Cao S M, et al. Ion microprobe zircon U-Pb age and geochemistry of the Myanmar jadeitite. J Geol Soc London, 2008, 165: 221—234[DOI]

9 Goffe B, Rangin C, Maluski H. Jade and associated rocks from the jade Mines area, Northern Myanmar as record of a polyphased high pressure metamorphism. J Asian Earth Sci, 2002, 20(suppl): 16—17

10 Zhang W J. Jadeite deposit geology in Pharkant area, North Myamar

(in Chinese). Yunnan Geol, 2002, 21: 378－390
11 Yu B. Research of development and thinking on the genesis of primary Feicui in Burma (in Chinese). Jewel Sci Tech, 2003, 15(5): 31－34
12 Zhang L J. Characteristics and genesis of the primary jadeite jade ore body in Nammaw, Myanmar (in Chinese). Acta Petrol Mineral, 2004, 23: 49－53
13 Qiu Z L, Chen B H, ZhangY. Enclave within jadeite and its significance for distinguishing A and B jade (in Chinese). Gems Jades China, 1996, 1: 56－57
14 Qiu Z L. The concept of inclusion in gemology and the category of jade enclave (in Chinese). Acta Sci Nat Uni SunYat-sen, 1998, (S1): 104－108
15 Peng Z L, Peng M S. Inclusions in jadeite from Burma (in Chinese). Acta Sci Nat Uni SunYat-sen, 2004, (4): 98－101
16 Shi G H, Cui W Y, Liu J, et al. Petrology of jadeite-bearing serpentinized peridotite and its country rocks from Northwestern Myanmar (Burma) (in Chinese). Acta Petrol Sin, 2001, 17: 483－490
17 Mo T. Geological character of jadeite deposit in Pharkant area of Burma. In: Wu R H, ed. New Researches About Burma Jadeite. Wuhan: China University Geoscience Press, 2003. 22－28
18 Barley M E, Pickard A L, Khin Z, et al. Jurassic to Miocene magmatism and metamorphism in the Mogok metamorphic belt and the India-Eurasian collision in Myanmar. Tectonics, 2003, 22: 1019－1029[DOI]
19 Morley C K. Nested strike-slip duplexes, and other evidence for Late Cretaceous-Palaeogene transpressional tectonics before and during India-Eurasia collision, in Thailand, Myanmar and Malaysia. J Geol Soc London, 161: 799－812
20 Acharyya S K. Collisional emplacement history of the Naga-Andaman ophiolites and the position of the eastern Indian suture. J Asian Earth Sci, 2007, 29: 229－242[DOI]
21 Mitchell A H G, Htay M T, Htun K M, et al. Rock relationships in the Mogok Metamorphic belt, Tatkon to Mandalay, central Myanmar. J Asian Earth Sci, 2007, 29: 891－910[DOI]
22 Zhong D L. Paleo-Tethys orogenic belt in Western Yunnan (in Chinese). Beijing: Science Press, 1998. 231
23 Curray J R. Tectonic and history of the Andaman sea region. J Asian Earth Sci, 2005, 25: 187－232[DOI]
24 Li P, Cui W Y. Discovery of a new species of jadeite (in Chinese). Acta Sci Nat Uni Pekinensis, 2004, 40(2): 241－246
25 Htein W, Naing A M. Mineral and chemical composition of jade of Myanmar. J Gem, 1994, 24: 269－276
26 Shi G H, Cui W Y, Wang C Q, et al. The fluid inclusions in jadeitite from Pharkant area, Myanmar. Chin Sci Bull, 2000, 45: 1896－1900[DOI]
27 Harlow G E, Sorensen S S. Jade (nephrite and jadeitite) and serpentinite: Metasomatic connections. Int Geol Rev, 2005, 47: 113－146[DOI]
28 Ao Y, Chen J. Compositions of different color jadeite from Burma (in Chinese). Jewelry Sci Tech, 1997, (4): 37－40
29 Huang F M, Gu Q H, Zou Y H. Mineral compositions and texture of jadeite jade and their relationships to quality types (in Chinese). J Gems Gemmol, 2000, 2(1): 7－14
30 Xie X, Wang D R, Wang C L. Discussion about colour of Burmese jadeite (in Chinese). J Xi'an Eng Uni, 2000, 22(4): 40－45
31 Yuan X Q. Jadeite Gemology (in Chinese). Wuhan: China University Geoscience Press, 2003
32 Di J G, Lu F D, Zhou S Y, et al. Elementary analysis of compositions and genesis on Kazakhstan jadeite (in Chinese). Jewelry Sci Tech, 2000, (2): 38－39
33 Chen K Q, Ma C X, Luan R J. On the relation between genesis and features of composition, texture and structure of Feicui (in Chinese). Yunnan Geol, 1998, 17(3-4): 350－355
34 Ouyang Q M, Qu Y H. Characteristic of western Sayan jadeite jade deposit in Russia (in Chinese). J Gems Gemmol, 1999, (1): 5—11
35 Xu P, Wu F Y, Xie L W, et al. Hf isotopic compositions of the standard zircons for U-Pb dating. Chin Sci Bull, 2004, 49: 1642－1648[DOI]
36 Wu F Y, Yang Y H, Xie L W, et al. Hf isotopic compositions of the standard zircons and baddeleyites used in U-Pb geochronology. Chem Geol, 2006, 234: 105－126[DOI]
37 Xie L W, Zhang Y B, Zhang H H, et al. *In situ* simultaneous determination of trace elements, U-Pb and Lu-Hf isotopes in zircon and baddeleyite. Chin Sci Bull, 2008, 53: 1565－1573[DOI]
38 Wu Y B, Zheng Y F. Genesis of zircon and its constraints on interpretation of U-Pb age. Chin Sci Bull, 2004, 49: 1554－1569[DOI]
39 Belousova E A, Griffin W L, O'Reilly S Y, et al. Igneous zircon: Trace element composition as an indicator of source rock type. Contrib Mineral Petrol, 2002, 143: 602－622
40 Hoskin P W O, Schaltegger U. The composition of zircon and igneous and metamorphic petrogenesis. In: Hanchar J M, Hoskin P W O, eds. Zircon. Rev Mineral Geochem, 2003, 53: 27－62[DOI]
41 Hoskin P W O. Trace-element composition of hydrothermal zircon and the alteration of Hadean zircon from the Jack Hills, Australia. Geochim Cosmochim Acta, 2005, 69: 637－648[DOI]
42 Pelleter E, Cheilletz A, Gasquet D, et al. Hydrothermal zircons: A tool for ion microprobe U-Pb dating of gold mineralization (Tamlalt-Menhouhou gold deposit-Morocco). Chem Geol, 2007, 245: 135－161[DOI]
43 Dubínska E, Bylina P, Kozlówski A, et al. U-Pb dating of serpentinization: hydrothermal zircon from a metasomatic rodingite shell (Sudetic ophiolite, SW Poland). Chem Geol, 2004, 203: 183－203[DOI]
44 Pettke T, Audétat A, Schaltegger U, et al. Magmatic-tohydrothermal crystallization in the W–Sn mineralized Mole Granite (NSW, Australia): Part II: Evolving zircon and thorite trace element chemistry. Chem Geol, 2005, 220: 191－213[DOI]
45 Wu F Y, Huang B C, Ye K, et al. Collapsed Himalaya-Tibetan orogen and the rising Tibetan Plateau. Acta Petrol Sin, 2008, 24: 1－30
46 Sorensen S S, Barton M D. Metasomatism and partial melting in a subduction complex: Catalina schist, southern California. Geology, 1987, 15: 115－118[DOI]
47 Morishita T A, Arai S, Ishida Y. Trace element compositions of jadeite (+ omphacite) in jadeitites from the Itoigawa-Ohmi district, Japan: Implications for fluid processes in subduction zones. Island Arc, 2007, 16: 40－56[DOI]
48 Wu F Y, Li X H, Zheng Y F, et al. Lu-Hf isotopic systematics and their applications in petrology. Acta Petrol Sin, 2007, 23: 185－220
49 Zheng Y F, Wu Y B, Zhao Z F, et al. Matamorphic effect on zircon Lu-Hf and U-Pb isotope systemsin ultra-high-pressure eclogite-facies metagranite and metabasite. Earth Planet Sci Lett, 2005, 240: 378－400[DOI]
50 Chu M F, Chung S L, Song B, et al. Zircon U-Pb and Hf isotope constraints on the Mesozoic tectonics and crustal evolution of Southern Tibet. Geology, 2006, 34: 745－748[DOI]
51 Zhang H F, Xu W C, Guo J Q, et al. Zircon U-Pb and Hf isotopic composition of deformed granite in the southern margin of the Gangdese belt, Tibet: Evidence for early Jurassic subduction of Neo-Tethyan oceanic slab (in Chinese). Acta Petrol Sin, 2007, 23: 1347－1353